IMA Journal of Mathematical Control and Information Page 1 of 31
doi:10.1093/imamci/dnnxxx

Distributed control of compact formations for multi-robot swarms

GABRIEL RODRIGUES DE CAMPOS [(1)], DIMOS V. DIMAROGONAS [(2)], ALEXANDRE SEURET [(3)], KARL H. JOHANSSON [(2)]

[(1)] *Politecnico di Milano, Italy.* ***Email: gabriel.rodriguesdecampos@polimi.it***

[(2)] *Royal Institute of Technology (KTH), Sweden.* ***Email: dimos, kallej@kth.se***

[(3)] *CNRS LAAS, Univ. de Toulouse, France.* ***Email: aseuret@laas.fr***

This paper proposes a distributed algorithm for the compact deployment of robots, using both distance- and angular-based arguments in the controllers' design. Our objective is to achieve a configuration maximizing the coverage of the environment while increasing the graph's connectivity. First, we provide: (i) a dispersion protocol guaranteeing connectivity maintenance; and (ii) a compactness controller with static and variable control gains that minimizes the inter-agent angles. Second, we present a sequential, multi-stage strategy and analyse its stability. Finally, we validate our theoretical results with simulations, where a group of robots are deployed to carry out sensing or communication tasks.

Keywords: Multi-agent systems (MAS), Dispersion, Compact formations, Formation shape control

1. Introduction

Increasing algorithmic sophistication and computational capabilities of intelligent, autonomous agents have enabled their application to complex tasks in different domains. The range of applications of multi-robot systems includes search and rescue missions, intelligent transportation systems, wireless surveillance networks, disaster relief operations, assisted living or military/police action support [Manathara *et al.* (2011)]. In each of these applications, inclusion of intelligent, autonomous agents and decision support systems can save costs, increase efficiency, and leave humans to deal with higher-level tasks. However, this requires harmonious and effective cooperation between the robots themselves and, in certain cases, between robots and humans. An illustrative example of a search and rescue operation is presented in Figure 1, where mobile robots/vehicles need to efficiently sweep an unknown environment while supporting the activities of a human operator.

The complexity of certain missions often requires vehicles to deploy over a region, assume a specified pattern, make a cooperative decision or move in a synchronized manner. Moreover, as the complexity of missions increases, robots may also be required to evolve in aggressive and time-varying environments. This requires control policies that guarantee increased dynamic reconfiguration capabilities, in order to ensure quality of service (QoS) and performance subject to communication and sensing constraints. All these challenges led the way to extensive studies on multi-agent systems (MAS) and their properties, spanning several scientific communities and focusing on a wide range of control, communication, sensing or computational problems. For instance, a large literature exists on situational awareness [Kruijff *et al.* (2014)], adversarial interactions and complexity management [Shamma (2007)] and motion coordination strategies [Martínez *et al.* (2007)] such as flocking protocols [Olfati-Saber (2006); Yao-Li *et al.* (2007)], consensus and rendezvous algorithms [Cortés *et al.* (2006); Dimarogonas *et al.* (2007); Seo *et al.* (2011); Shen *et al.* (2012); Rodrigues de Campos *et al.* (2011, 2012)] or formation control [Egerstedt *et al.* (2001); Dong (2011); Wen *et al.* (2013); Sun *et al.* (2015)].

The author 2008. Published by Oxford University Press on behalf of the Institute of Mathematics and its Applications. All rights reserved.

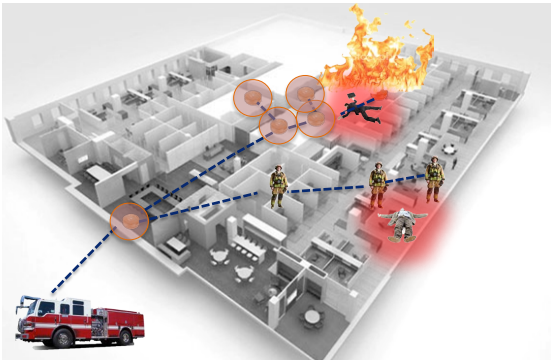


FIG. 1. An illustrative example of a search-and-rescue scenario, where a team of humans and autonomous agents needs to accomplish a task. For the sake of the success of the mission, the autonomous agents need to efficiently sweep an unknown, aggressive environment while keeping communication links among themselves and the human players. For such scenarios, increased connectivity properties are crucial from an efficiency, safety and redundancy point of view.

1.1 *Related research*

In the sequel, we provide a selection of results related to scope of this article. This section is articulated around two research topics: agent's deployment and formation shape control.

1.1.1 *Deployment, coverage and dispersion:* In the literature, a particular attention has been given to the coverage problem, firstly defined in [Gage (1992)]. From this initial work, different solutions have been proposed, for instance, to the visibility problem, i.e., where the part of the terrain that is monitored (visible) by the robot team has to be maximized [Mei *et al.* (2006); Hexsel *et al.* (2011)]. Among others, [Batalin *et al.* (2002, 2007)] used local dispersive interaction between robots to achieve good global coverage and [Howard *et al.* (2002)] considered an incremental algorithm which incorporates the maximum monitoring distance. On the other hand, the intervention problem, i.e., where the robot has to be as close as possible form every point in the terrain, is also adapted to several practical applications. This problem was firstly studied in [Cortés *et al.* (2004)], and a great number of solutions have been proposed since then for a variety of different scenarios [Schwager *et al.* (2009); Poduri *et al.* (2004)].

Some other works exploited the concept of cohesiveness, which can be characterized by a repulsion/attraction function that maintains desired relative distances between an agent and its neighbors [Olfati-Saber (2006); Mastellone *et al.* (2008)]. A continuous-time model for swarm aggregation is presented in [Gazi *et al.* (2003)], where it is proved that a group of agents form a cohesive swarm if each pair is subject to a potential function. In contradiction, other results focused on the inverse agreement problem or, in other words, in swarm dispersion [Dimarogonas *et al.* (2009)]. Here, each agent follows a potential field leading the swarm to a configuration where the minimum distance between the swarm members is identical. The same idea of artificial potential functions was also used for studying behavior-based control as in, e.g., [Cao *et al.* (2003); Donald *et al.* (2000); Reif *et al.* (1999)], as well as air traffic and road traffic control [Fankhauser *et al.* (2011); Makarem *et al.* (2012)].

Finally, other works focused on the connectivity maintenance problem [Zavlanos *et al.* (2008); Ji *et al.* (2007); Dimarogonas *et al.* (2010); Schuresko *et al.* (2009)], where (often distributed) coordination

algorithms allow robots to adapt their motion profiles so to preserve connectivity. More recently, [Bezzo *et al.* (2010, 2011a,b)] tackled the deployment of mobile routers in accident areas problem, using an appropriated routing and position optimization algorithm.

1.1.2 *Formation shape control* A fundamental task for robot reconfiguration is formation shape control. The reader can refer to [Oh *et al.* (2015)] for a recent survey on multi-agent formation control.

By definition, the formation shape control problem involves a group of agents tasked with forming and maintaining a given geometric shape, described in terms of relative geometrical constraints. Among many others, [Bishop *et al.* (2015); Mou *et al.* (2015)] have recently proposed distributed control strategies guaranteeing the convergence to a prescribed formation shape, while [Martínez *et al.* (2006)] proposed different approaches to deal with location and trajectory following of a moving target. Formation control based on virtual structure methods was also introduced in [Chen *et al.* (2010); Consolinia *et al.* (2008); Beard *et al.* (2001)] and strategies especially tailored to submarine/oceanic applications were studied in, e.g., [Sepulchre *et al.* (2008); Brinon-Arranz, *et al.* (2014); Ghabcheloo *et al.* (2005)], with an emphasis on circular formations. Recently, [Eren (2012)] also exploited rigid graph theory for bearing-based formation control.

Closer to the topic of this paper, some other works focused on the formation shape control of triangular formations. In [Cao *et al.* (2007)], a "positively-oriented" triangular formation is maintained by having each agent locally controlling its own position so that the distance to the next agent in the triangle is constant. This approach was later extended in [Cao *et al.* (2011)] to a multi-level procedure, where each agent cyclically switches between periods of localization, position control and standby. A distance based approach was also considered in [Summers *et al.* (2009); Anderson *et al.* (2010)], where authors analyse equilibrium formation shapes with incorrect interagent distances. In a different way, [Basiri *et al.* (2010); Bishop (2011a); Bishop *et al.* (2011b, 2010)] consider an angle-based (rather than inter-distance based) perspective. Here, each agent measures the bearing to the other two agents in a local coordinate system, and control its motion according to prescribed geometric constraints.

1.2 *Problem formulation and contribution statement*

In this paper, we focus on the problem of the compact deployment of vehicles, so to improving the communication linkage among the swarm members. This work is motivated by applications requiring the deployment of a group of robots to carry out sensing (i.e., mobile sensors) and communication (i.e., mobile routers) tasks, as illustrated in Figure 1. Such scenarios have also been recently considered in, e.g., the DARPA LANdroids program. We pay a particular attention to the graph's connectivity, which is an useful or even necessary property for multi-robot systems. For instance, higher connectivity offers great advantages if one aims to perform agreement procedures over a set of robots/sensors, as the connectivity of a graph greatly influences the speed of convergence of such protocols. Also, other applications may ask for redundancy on measurements, especially when critical decisions are dependent on it.

Our goal is to achieve a (static) configuration maximizing the coverage of the environment while achieving and maintaining high connectivity. The three problems tackled are defined as follows:

- Deployment/coverage/dispersion:
  - **PROBLEM 1- Dispersion:** Given a set of N agents operating in the workspace $W \subset \mathbb{R}^2$, find local control policies such that each agent is separated by a given, fixed distance from all its neighbours.

  - **PROBLEM 2- Connectivity maintenance:** Given a set of N agents operating in the workspace $W \subset \mathbb{R}^2$, find local control policies such that initially existing communication links do not vanish/break as time evolves.

- Formation shape control:

  - **PROBLEM 3- Compactness:** Given a set of N agents operating in the workspace $W \subset \mathbb{R}^2$, find local control policies minimizing the inter-agent angles, so to increase the number of communication links.

The major algorithmic contribution of this paper is the development of a distributed law for angular-constrained formation control of a multi-agent system under sensing/communication constraints. Unlike common solutions, which use either distance-based or angle-based constraints, we propose here a novel perspective coupling these two approaches in the design of the controllers.

The features of the suggested solution are given as follows. To solve Problems 1 and 2, a potential field based approach is proposed, which is inspired from the results of [Dimarogonas *et al.* (2009)]. More precisely, each agent is equipped with potential functions that will, simultaneously, isolate it from any other agent and impose connectivity maintenance using only information of those located within its sensing zone. Regarding Problem 3, we base our approach on the inter-agent angles formed within the formation, that should be minimized in order to achieve compact configurations. See Figure 2 for an illustration. As considered in this paper, the desired of compactness notion stems from the optimal connectivity properties of a three-agent network. Generally speaking, it follows that a compact configuration presents a triangular-based pattern, where for each triplet the (smallest) inter-agent angles is minimized, as shown Figure 2. Note that minimizing the inter-agent angles comes to maximizing the node degree (the number of neighbors of each node). This work is motivated by the vast literature on bearing-only state estimation and localization and the applications of optimal sensor arrangement solutions. This makes angle-based formation control particularly appealing, especially considering that angle-based approaches are still rare in the literature.

The contributions of this paper can finally be summarized as follows. First, we present a distributed control strategy, where each mobile sensor makes decisions based only on the limited information from its neighbors. Coordination is enforced through simple yet effective control laws, in opposition to more complex optimization-based approaches. Second, we relax the assumptions on the initial configuration and sensing/communication graph. Unlike [Summers *et al.* (2009); Anderson *et al.* (2010)], that require a all-to-all communication graph, or [Basiri *et al.* (2010); Cao *et al.* (2007)] that assume the

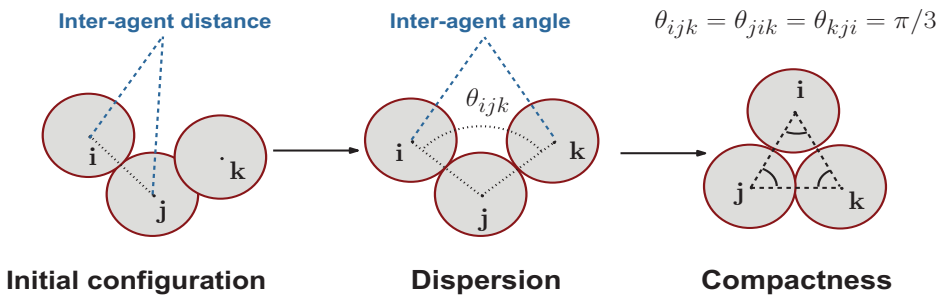


FIG. 2. Illustration of the control objectives

existence of an initially formed triangular configuration, we show here how one can achieve a compact, triangular-based configuration even if there is no triangular sensing pattern at time zero. Finally, and most important, our results hold for configurations of four agents, and for which formal stability properties are derived. The case of a three agent network, as commonly considered in literature [Cao *et al.* (2007); Basiri *et al.* (2010); Bishop (2011a)], is a particular case of the systems considered in this manuscript. Most important, the above mentioned papers fail to handle most of the scenarios considered here, due to their assumptions on the initial configuration. This is discussed later in Section 6.3. To the best of the authors knowledge, no similar results on provably stable, angle-based formation control with connectivity constraints exist in the literature for systems with more than three agents.

The rest of the paper is organized as follows: Section 2 describes the system and important concepts/definitions. Section 3 and 4 deal with controller design and stability analysis for the dispersion and compactness algorithms, respectively, while Section 5 provides a sequential controller. Finally, Section 9 includes simulation results and Section 7 presents our conclusions and perspectives for future research.

2. System and framework definition

2.1 *Notation*

Throughout the paper, $\mathbb{R}^n$ denotes the n-dimensional Euclidean space, and $\mathbb{R}^{n\times m}$ is the set of $n\times m$ real matrices. The matrix I_n represents the identity matrix of $\mathbb{R}^{n\times n}$. Finally, for any matrix $M\in\mathbb{R}^{n\times n}$, the notation $(M)_i$ denotes the i^{th} row of M, $(M)_{ij}$ the element on the i^{th} row and j^{th} column of M, $\lambda_k(M)$ the k^{th} eigenvalue of M and M^T the transpose of M. Moreover, $\otimes$ stands for the standard Kronecker product between two matrices. Also, R_{ot} is the rotation matrix of $\pi/2$ radians on the clockwise direction.

2.2 *System Description*

Take N agents operating in the workspace $W\subset\mathbb{R}^2$. We consider that the motion of each agent is described by single integrator dynamics[1], as commonly used in literature [Cao *et al.* (2007), Dimarogonas *et al.* (2009), Pavone & Frazzoli (2006)]. Note that other common modelling choices for multi robot-control also include, for example, double-integrator dynamics [Deshpande *et al.* (2011), Cao *et al.* (2011), Ren *et al.* (2008)] or unicycle kinematic models [Dimarogonas *et al.* (2007); Bishop (2011a); Basiri *et al.* (2010)]. We then have:

$$\dot{q}_i = u_i,\ \ i\in\mathcal{N}=\{1,...,N\}, \tag{2.1}$$

where $q_i\in\mathbb{R}^2$ denotes agent i position, $q=[q_1^T,...,q_N^T]^T$ represents the agents configuration, and u_i the control input for each agent. Define also the vector connecting any two agents (i,j) as:

$$q_{ij}=q_j-q_i,$$

and β_{ij} as the squared distance between two agents given by:

$$\beta_{ij}=\|q_j-q_i\|^2,\forall\, i,j\in\mathcal{N}. \tag{2.2}$$

[1]Note that simple integrator dynamics can be considered for trajectory generation and used in a trajectory-tracking setup for controlling more complex systems.

Throughout this article, we denote for $i \in \mathscr{N}$ and $d > 0$:

$$\mathscr{N}_{i,d}(t) = \left\{ j \in \mathscr{N} \backslash \{i\} |\ \ \beta_{ij} \leqslant d^2 \right\},$$

as the subset of $\mathscr{N}$ including all neighbors of agent i, *i.e.*, all nodes that agent i can sense within a radius $d/2$. Moreover, $|\mathscr{N}_{i,d}|$ denotes the number of neighbors of agent i. Define for each agent i a d-proximity graph as:

$$\mathscr{P}_{i,d}(t) = \left(\mathscr{N}_{i,d}(t), \Upsilon_i(t)\right),$$

where $\Upsilon_i(t) \subseteq \mathscr{N}_{i,d}(t) \times \mathscr{N}_{i,d}(t)$ is the set of edges connecting agent i to all $j \in \mathscr{N}_{i,d}$ at time t.

In the sequel, each agent is suppose to have two (common) overlapping sensing radii such that $d_1 < d_2$, see Figure 3. It follows that:

$$d_1 = \xi d_2,$$

where $0 < \xi \leqslant 1$. Note that $1/\xi$ can be viewed as a safety factor: the larger its value, the smaller the probability of losing an edge is. It is worth mentioning that the use of two overlapping communication radii is strictly related to the problems treated in this article. We recall that the objective of our controllers is: **(i)** to separate agents without losing communication and **(ii)** to achieve a compact deployment by controlling the inter-agent angles. Therefore, the smaller radius d_1 bounds the area wherein the inter-agent distances are controlled, while d_2-proximity graphs are used to establish a larger domain wherein we control the inter-agent angles.

2.3 *Definitions and assumptions*

We introduce the following definitions and assumptions for a triplet (i, j, k).

DEFINITION 2.1 A triplet $(i, j, k) \in \mathscr{N}^3$ is a *Connected Triplet* if i, j, k are all distinct and

$$i, k \in \mathscr{N}_{j,d_2},\ i \notin \mathscr{N}_{k,d_2}.$$

Thus, a Connected Triplet is a connected graph, where the central vertex can sense the other two agents, while the other two can only sense the central agent. Note that, in terms of notation, the order of agents matters. This means that, when Connected Triplets are discussed, a triplet (i, j, k) is centered at j.

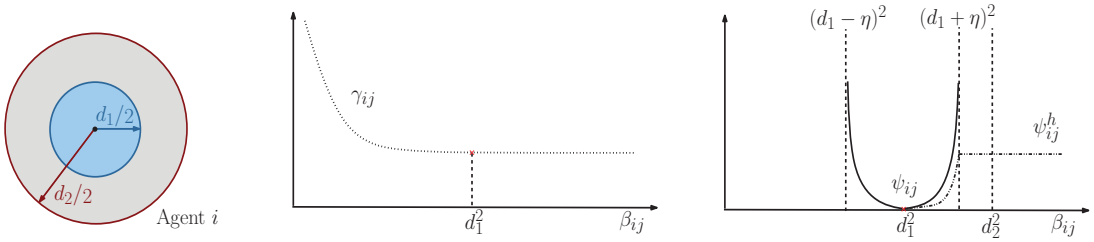


FIG. 3. Communication radii and potential functions

DEFINITION 2.2 A triplet $(i,j,k) \in \mathscr{N}^3$ is a *Complete Triplet* if i,j,k are all distinct and

$$i,k \in \mathscr{N}_{j,d_2},\ i \in \mathscr{N}_{k,d_2}.$$

Then, it follows that a Complete Triplet is a three nodes complete graph.

Throughout this article, we will often refer to the angle formed by a given *Connected Triplet* (i,j,k), also called *inter-agent angle*. For the sake of clearness of the presentation, the following definition is introduced.

DEFINITION 2.3 A *Connected Triplet* (i,j,k), where j is the central agent from a geometric point of view, defines the *inter-agent angle* θ_{ijk} such that:

$$\theta_{ijk} = \arccos\left(\frac{<q_{ji},q_{jk}>}{\|q_{ij}\|\cdot\|q_{jk}\|}\right), \tag{2.3}$$

where $\|.\|$ represents the Euclidean norm and $<.>$ the scalar product.

An illustrative example of an *inter-agent angle* is depicted in Figure 4. The following assumption holds.

ASSUMPTION 2.1 For any inter-agent angles θ_{ijk}, where the $(i,j,k) \in \mathscr{N}^3$ is a Connected Triplet according to Definition 2.1, we assume that $cos(\theta_{ijk}) \neq 1$ or, in other words, that $\theta_{ijk} \neq k\pi,\ k \in \{0,1,2,\ldots\}$.

In the scope of this article, the notion of an inter-agent angle stands for the angle with the smaller absolute value formed by a Connected Triplet $(i,j,k) \in \mathscr{N}^3$. The previous assumption is introduced such that inter-agent angles are well-defined. Hence, angles θ_{ijk} for which $cos(\theta_{ijk}) = 1$ are naturally excluded. Note that similar assumptions, on non-collinear triangular formations, are also considered and discussed in [Cao *et al.* (2007)], and identically in [Bishop (2011a); Basiri *et al.* (2010)].

3. Dispersion Algorithm

In this section, we propose a potential field-based controller for agents' dispersion.

3.1 *Preliminaries*

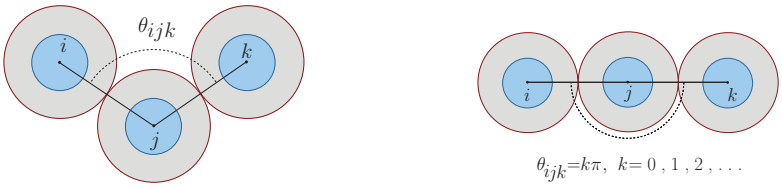
Given a swarm composed of an arbitrary number of agents, let:

$$\mathscr{I}(d_1) = \left\{q \in W \mid \forall i \in \mathscr{N}, \forall j \in \mathscr{N}_{i,d_2},\ 0 < \beta_{ij} \leqslant d_1^2\right\},$$

denote the set of feasible initial conditions[2]. Take η as an integer, user-defined parameter defining a close neighborhood of d_1 such that $d_1 + \eta < d_2$, see Figure 3. Then, the set of desired, final configurations for the dispersion protocol should satisfy the following condition:

$$\mathscr{F}(d_1,\eta) = \left\{q \in W \mid \forall i \in \mathscr{N}, \forall j \in \mathscr{N}_{i,d_2},\ (d_1-\eta)^2 < \beta_{ij} < (d_1+\eta)^2\right\}.$$

[2]The set $\mathscr{I}(d_1)$ has been specifically defined for the two-layered strategy presented later in this paper. Nevertheless, if the dispersion controller is considered independently, the assumptions on the initial configuration can be relaxed to any configuration satisfying $\beta_{ij} > 0,\ \beta_{ij} \neq (d_1 \pm \eta)^2,\ \forall i \in \mathscr{N}, \forall j \in \mathscr{N}_{i,d_2}$.



(a) (b)

FIG. 4. For a *Connected Triplet* (i,j,k), and according to Definition 2.3, an illustration of: (a) a valid *inter-agent angle* and (b) an invalid *inter-agent angle*.

In this section, we focus on inverse agreement protocols, using a potential-field approach to ensure agents' dispersion. We based our approach on the results of [Dimarogonas *et al.* (2009)], and improve them by using additional fields to guarantee connectivity maintenance. Consider Figure 3, where the potential function γ_{ij} guaranteeing dispersion is illustrated. The key features of this function are described as follows:

Definition of the potential function γ_{ij} for a couple of distinct agents $(i,j) \in \mathcal{N}^2$:

- γ_{ij} is a decreasing function, twice continuously differentiable
- γ_{ij} tends to $+\infty$ when β_{ij} tends to zero.
- $\frac{\partial \gamma_{ij}}{\partial \beta_{ij}} = 0$ if $\beta_{ij} \geqslant d_1^2$.

In [Dimarogonas *et al.* (2009)], it has been shown in that a control strategy based on γ_{ij} will lead to a configuration in which the minimum distance between any pair of agents is larger than a specific lower bound, equal to the agents' sensing radius. However, function γ_{ij} cannot guarantee connectivity maintenance on itself. In order to tackle this problem, we introduce in this paper a new, additional function $\psi_{ij} \in C([0,+\infty))$, also illustrated in Figure 3. Note that η is a positive scalar defining the size of the desired neighborhood for connectivity maintenance. The function ψ_{ij} is defined such that:

Definition of the potential function ψ_{ij} for a couple of distinct agents $(i,j) \in \mathcal{N}^2$:

- ψ_{ij} tends to ∞ when β_{ij} tends to $(d_1 \pm \eta)^2$.
- $\psi_{ij} = 0$ and $\frac{\partial \psi_{ij}}{\partial \beta_{ij}} = 0$ if $\beta_{ij} = d_1^2$.

Given its bounding characteristics, ψ_{ij} is particularly adequate to cases where the considered communication graph is static, that is, when no new edges are added whenever an agent, not initially located within the sensing zone of another agent, enters this zone. In practical situations, however, it is useful to consider the creation of new edges whenever an agent enters the sensing zone of another robot. Hence, we define ψ_{ij}^h that ensures a smooth transition to ψ_{ij} such that:

Definition of the additional potential function ψ_{ij}^h for a couple of distinct agents $(i,j) \in \mathscr{N}^2$:

- ψ_{ij}^h is differentiable everywhere
- $\psi_{ij}^h = 0$ and $\frac{\partial \psi_{ij}^h}{\partial \beta_{ij}} = \frac{\partial \psi_{ij}}{\partial \beta_{ij}}$ when $\beta_{ij} = d_1^2$.
- ψ_{ij}^h is strictly increasing when $d_1^2 < \beta_{ij} < (d_1+\eta)^2$.
- ψ_{ij}^h is constant when $\beta_{ij} > (d_1+\eta)^2$.

Through the remaining of the paper, the subset of the sensing zone of agent i including all agents that form a new edge with agent i will be defined as:

$$\mathscr{N}_{i,d_1+\eta}^h = \left\{ j \in \mathscr{N} \backslash \{i\},\ \beta_{ij} < (d_1+\eta)^2,\ \dot{\beta}_{ij} < 0 \right\}.$$

Finally, let us present here LaSalle's Invariance Principle.

THEOREM 3.1 **LaSalle's Invariance Principle [Khalil (2015)]:** Let $\Omega \subset D$ be a compact set that is positively invariant with respect to $\dot{x} = f(x)$. Let $V : D \to R$ be a continuous differentiable function such that $\dot{V}(x) \leqslant 0$ in Ω. Let E be the set of all points in Ω such that $\dot{V}(x) = 0$. Let M be the largest invariant set in E. Then every solution starting in Ω approaches M as $t \to \infty$.

3.2 *Controller Design*

In the sequel, we present the dispersion controller denoted by u_1, whose structure is illustrated in Figure 5. For each communicating pair of agents (i,j), γ_{ij} is active implying that agents will diverge from each other (*Dispersion*). Designed to keep connectivity (*Confinement*), ψ_{ij} becomes active at t_{ij}^*, where:

$$t_{ij}^* = \min\{t |\ \beta_{ij}(0) < d_1^2, \beta_{ij}(t) = d_1^2,\ \forall i \in \mathscr{N},\ \forall j \in \mathscr{N}_{i,d_1}\}. \tag{3.1}$$

This means that t_{ij}^* represents the instant for which the distance between two agents i and j, initially closer than d_1 and such that $\dot{\beta}_{ij} > 0$, reach for *the first time* the threshold distance d_1. Consequently, the instant for which the length of an edge of the overall network reaches the threshold distance d_1, for *the first time*, is defined as:

$$t_a^* = \min\ \{t |\ \text{eq. (3.1) is satisfied}\},$$

and corresponds to the smallest value of all t_{ij}^* among all pairs $i,j \in \mathscr{N}$ for which $\beta_{ij}(0) < d_1^2$. The structure of our approach is illustrated in Figure 5, presenting the controller sequence regarding the evolution of both time and β_{ij}. For any pair of agents (i,j) for which $\beta_{ij}(0) < d_1^2$, the dispersion controller is applied while $t < t_{ij}^*$. Then, the connectivity maintenance controller takes over for all $t > t_{ij}^*$, whenever $\beta_{ij} < (d_1+\eta)^2$.

The partial derivative of the potential functions can be computed as $\partial \gamma_{ij}/\partial q_i = 2\frac{\partial \gamma_{ij}}{\partial \beta_{ij}}(D_{ij})_i q$, $\partial \psi_{ij}/\partial q_i = 2\frac{\partial \psi_{ij}}{\partial \beta_{ij}}(D_{ij})_i q$, and their gradient as $\nabla \gamma_{ij} = 2\frac{\partial \gamma_{ij}}{\partial \beta_{ij}} D_{ij} q$ and $\nabla \psi_{ij} = 2\frac{\partial \psi_{ij}}{\partial \beta_{ij}} D_{ij} q$,

where the matrix D_{ij} is given as:

$$D_{ij} = \bar{D}_{ij} \otimes I_2,$$

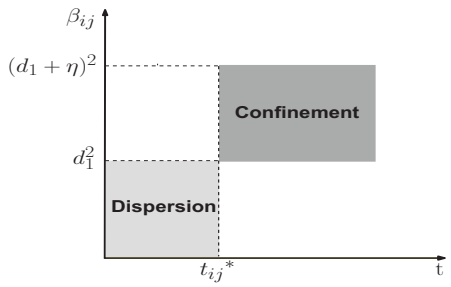


FIG. 5. Dispersion controller's time schedule for any initially close pair of agents (i, j)

with $\bar{D}_{ij} \in \mathbb{R}^{N\times N}$ such that $\bar{D}_{ii} = 1$, $\bar{D}_{ij} = -1$ and all other terms are equal to zero. Thus, the proposed controller can be expressed as:

$$u_{i1} = -\sum_{j\in\mathcal{N}_{i,d_1}} \frac{\partial \gamma_{ij}}{\partial q_i} - \sum_{j\in\mathcal{N}^h_{i,d_1+\eta}} \frac{\partial \bar{\psi}_{ij}}{\partial q_i} - \sum_{j\in\mathcal{N}_{i,d_2}} \frac{\partial \bar{\psi}^h_{ij}}{\partial q_i}. \tag{3.2}$$

In the previous equation, $\bar{\psi}_{ij}$ and $\bar{\psi}^h_{ij}$ are given by:

$$\bar{\psi}_{ij}(t) = \begin{cases} 0, & \text{if } t < t^*_{ij}, \\ \psi_{ij}, & \text{otherwise,} \end{cases} \qquad \bar{\psi}^h_{ij}(t) = \begin{cases} \psi^h_{ij}, & \text{if } t < t^{**}_{ij}, \\ \psi_{ij}, & \text{otherwise ,} \end{cases}$$

where

$$t^{**}_{ij} = \min\{t|\ \beta_{ij}(0) > d_2^2, \dot{\beta}_{ij} < 0, \beta_{ij}(t) = d_1^2,\ \forall i \in \mathcal{N},\ \forall j \in \mathcal{N}^h_{i,d_1+\eta}\}.$$

It is worth mentioning that according to previous definitions, both $\bar{\psi}_{ij}(t)$ and $\bar{\psi}^h_{ij}(t)$ are continuous with respect to β_{ij} and $\dot{\beta}_{ij}$. Furthermore, note that the function $\bar{\psi}^h_{ij}$ is defined such that it switches, in a smooth way, from ψ^h_{ij} to ψ_{ij} whenever an agent j forms a new edge with agent i. The reader should refer to Section 3.1 for the definitions of ψ_{ij} and ψ^h_{ij}.

Knowing that equation (3.2) corresponds to the sum of the negative gradients of the potential functions, this yields that each agent is then subject to both a repulsive and attractive force with respect to any other agent within its sensing zone. Define now:

$$\psi^H_{ij} = \begin{cases} \bar{\psi}^h_{ij}, & \text{if } j \in \mathcal{N}^h_{i,d_1+\eta}, \\ \bar{\psi}_{ij}, & \text{otherwise ,} \end{cases}$$

and

$$\sigma^H_{ij} = \begin{cases} \frac{\partial \bar{\psi}^h_{ij}}{\partial \beta_{ij}}, & \text{if } j \in \mathcal{N}^h_{i,d_1+\eta}, \\ \frac{\partial \bar{\psi}_{ij}}{\partial \beta_{ij}}, & \text{otherwise .} \end{cases}$$

We then have:

$$u_1 = -2\left[R_1 \otimes I_2 + R_2 \otimes I_2\right] q, \tag{3.3}$$

where R_1 and R_2 are $N \times N$ matrices defined as:

$$(R_1)_{pq} = \begin{cases} \sum\limits_{j \in \mathcal{N}\setminus\{p\}} \dfrac{\partial \gamma_{pj}}{\partial \beta_{pj}}, & \text{if } p = q, \\ -\dfrac{\partial \gamma_{pq}}{\partial \beta_{pq}}, & \text{otherwise.} \end{cases} \qquad (R_2)_{pq} = \begin{cases} \sum\limits_{j \in \mathcal{N}\setminus\{p\}} \sigma^H_{pj}, & \text{if } p = q, \\ -\sigma^H_{pq}, & \text{otherwise.} \end{cases}$$

3.3 *Stability Analysis*

This section provides a stability analysis for the dispersion algorithm. The proposed controller ensures the deployment of all agents in the workspace while preserving connectivity (i.e., avoiding loosing edges). The next result holds for any number N of agents. For the sake of clarity of the presentation, all proofs are presented at the end of the paper.

THEOREM 3.2 Consider $N > 0$ agents described by (2.1) and driven by control law (3.2). Assume a set of feasible initial conditions $\mathscr{I}(d_1)$. Then the system reaches a final static configuration belonging to $\mathscr{F}(d_1, \eta)$.

Proof. The complete proof is presented in the appendix, Section 9.1. □

In this section, we presented a potential field-based controller for the deployment of agents. We have proved its efficiency and stability, for any value of the number of agents N, η or ξ. It is worth mentioning that the use of attraction/repulsion potential fields or, more generally, navigation functions, offers two main benefits. Firstly, decentralized navigation functions show a considerably low complexity with respect to the number of agents. Secondly, it is possible to combine them with different, more realistic dynamic models.

4. Compactness Controller

In order to appropriately deploy a group of agents able to carry out sensing and communication tasks, we focus our attention on the compactness of the swarm. More precisely, our approach is based on the minimization of the inter-agent angles. We aim at achieving compact formations composed of equilateral triangles, which inherently means that each angle should be equal to $\frac{\pi}{3}$. Considering this value as a reference, the proposed compactness controller relies on a force proportional to the difference between the angle value and the reference, that is applied to each Connected Triplet. Note that this force lies on a perpendicular direction of q_{ij}, denoted $q_{ij}^{\perp}$.

Motivated by applications where geometrical and connectivity/communication aspects of the formation are crucial for the success of the mission, we provide in the sequel results for four-agents networks, as a proof of concept of our strategy.

4.1 *Preliminaries*

The following assumption is introduced.

ASSUMPTION 4.1 We assume that η et ξ are, respectively, sufficiently close to 0 and 1. This inherently means that, upon dispersion, the distance separating two neighbors is taken to be constant and equal to d_1.

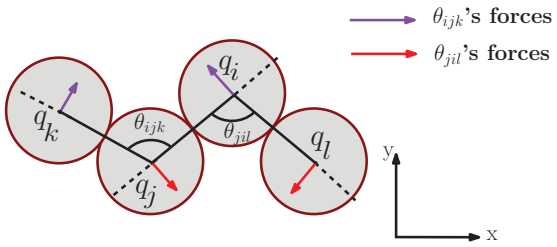


FIG. 6. Configuration of four agents

Let configurations where all Connected Triplets have two equal edges of length d_1 belong to:

$$\mathscr{E}(d_1) = \left\{ q \in W \mid \text{ for all Connected Triplets } (i,j,k),\ \beta_{ij} = \beta_{jk} = d_1^2 \right\}.$$

Furthermore, define the set including all configurations where each agent has at most Δ neighbors in d_2 - proximity graph as:

$$\mathscr{D}(d_2,\Delta) = \left\{ q \in W \mid \forall i \in \mathscr{N}, |\mathscr{N}_{i,d_2}| \leqslant \Delta \right\},$$

where Δ is a positive user-defined integer. Moreover, let set of feasible initial conditions be given as:

$$\mathscr{F}'(d_1,d_2) = \mathscr{D}(d_2,2) \cap \mathscr{E}(d_1), \tag{4.1}$$

and the a set of desired configurations as:

$$\mathscr{G}(d_1,d_2) = \left\{ q \in W \mid \forall j \in \mathscr{N}, \exists (i,k) \in \mathscr{N}^2_{j,d_2} \quad \text{st. } \beta_{ij} = \beta_{jk} = \beta_{ki} = d_1^2 \right\},$$

where all triplets (i,j,k) are Complete Triplets. Throughout the sequel, and unless told otherwise, we will consider a network of $N = 4$ agents with $\Delta = 2$, i.e., vehicles have at most two neighbors. A relaxation of these assumptions is currently ongoing work. We are now ready to present our control strategy for compactness control. The rest of this section is divided in two parts: the first part considers static control gains, while the second uses adaptive control gains in order to cope with singular configurations.

4.2 *Compactness Controller with Constant Gains*

4.2.1 *Controller Design* The underlying concept of our control strategy relies on a force, proportional to the difference between the angle value and the chosen reference, that is applied in a perpendicular direction of q_{ij}, denoted $q_{ij}^{\perp}$. More precisely, using the physical and mechanical concepts relating the applied force and the error regarding the equilibrium position of the system, a force proportional to difference between the actual angle value and the desired one is applied to the concerned agents. An illustration of this concept is presented in Figure 6.

For each agent i, the local compactness controller is then given as:

$$u_{i2} = -\sum_{i \in \mathscr{N}} \sum_{j \in \mathscr{N} \setminus \{i\}} \sum_{k \in \mathscr{N} \setminus \{i,j\}} \chi_{ijk} R_{ot} q_{ji}, \tag{4.2}$$

with

$$\chi_{ijk} = \begin{cases} K[\theta_{ijk} - sign(\theta_{ijk})\dfrac{\pi}{3}], & \text{if } (i,k) \in \mathscr{N}^2_{j,d_2} \setminus \mathscr{N}^2_{j,d_1}, \\ 0, & \text{otherwise,} \end{cases}$$

where K is a positive and constant gain. Rewritten in vector form, equation (4.2) yields:

$$u_2 = -\left[(R_3 \otimes I_2) R_{ot}\right] q, \tag{4.3}$$

where

$$(R_3)_{pq} = \begin{cases} \displaystyle\sum_{j \in \mathcal{N}\setminus\{p\}} \sum_{k \in \mathcal{N}\setminus\{p,j\}} \chi_{pjk}, & \text{if } p = q, \\ \displaystyle\sum_{k \in \mathcal{N}\setminus\{p,q\}} \chi_{pqk}, & \text{otherwise.} \end{cases}$$

By acting directly over the geometrical structure of the formation, we will show that controller (4.2) is able to improve the compactness of the swarm. Note that the value of the inter-agent angle within a triplet can only be computed by the central vertex, which can transmit this information to its neighbors. Hence, each robot decisions are only based on the limited information provided by its neighbors, see equation (4.2), without the existence of a formal central node or leader vehicle. Therefore, the distributed nature of our approach remains unchanged.

4.2.2 *Stability Analysis* The following results hold. Note that, for the sake of the clarity of the presentation, all the proofs are presented at the end of the article.

THEOREM 4.1 Consider $N = 4$ agents described by (2.1), denoted by (i, j, k, l) and driven by control law (4.2). Note that i and j are central vertices. Assume that the set of initial conditions is $\mathscr{F}'(d_1, d_2)$. Then the system reaches a final configuration belonging to $\mathscr{G}(d_1, d_2)$.

Proof. The complete proof is presented in the appendix, Section 9.2. □

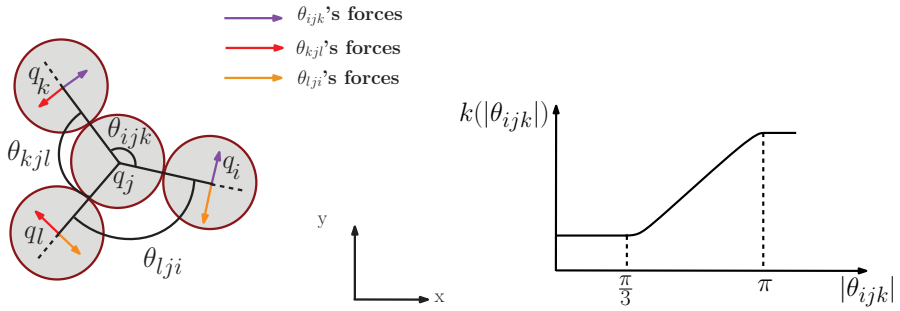
THEOREM 4.2 Consider $N = 4$ agents described by (2.1), denoted by (i, j, k, l) and driven by control law (4.2). Furthermore, assume an initial configuration as depicted in Figure 7(a), belonging to $\mathscr{I}'(d_1, d_2) = \mathscr{D}(d_2, 3) \cap \mathscr{E}(d_1)$, such that $\Delta = 3$ and where agent j is assumed to be central vertex. Then the system reaches a final configuration where the absolute values of all inter-agent angles $\theta_{ijk}, \theta_{lji}, \theta_{kjl}$ are equal to $2\pi/3$.

Proof. The complete proof is presented in Section 9.3. □

THEOREM 4.3 Consider $N = 3$ agents described by (2.1), denoted (i, j, k), and driven by control law (4.2). Assume the set of initial conditions $\mathscr{F}'(d_1, d_2)$, where j is the central vertex. Then the system reaches a final configuration belonging to $\mathscr{G}(d_1, d_2)$.

Proof. The complete proof is presented in the appendix, Section 9.4. □

Previous results exploit the concept of compactness, stemming from the ideal connectivity properties of a three-agent network, as shown in Figure 2. As a particular case of Theorem 4.1, the evolution of a three-agent configuration was also studied in Theorem 4.3. It seems however clear that the original configuration of the swarm plays an important role over the stability properties of the algorithm. As the results of Theorem 4.2 indicate, there exist indeed certain configurations that can lead the system to undesired equilibria. More precisely, Theorem 4.2 shows that a four-agent swarm, in an initial configuration as presented in Figure 7(a), will eventually reach a final configuration where $|\theta_{ijk}|, |\theta_{lji}|$, and $|\theta_{kjl}|$ are equal to $2\pi/3$. This can in fact be explained by a perfect balance of the forces applied to each agent, i.e., the sum of the vectorial contributions of each term of (4.2) is null such that $u_i = 0, \forall i \in \mathcal{N}$.



(a) Singular formation (b) Variable gain $k(|\theta_{ijk}|)$

FIG. 7. Illustration of a singular configuration and the representation of $k(|\theta_{ijk}|)$

4.3 *Compactness Controller with Variable Gains*

In order to avoid singular equilibrium and to generalize the previous results so to cope with singular formations, we propose in the sequel a control solution based on adaptive and variable gains.

4.3.1 *Controller Design*

Consider $K(\theta_{ijk})$ as an angle-dependent gain and defined as:

$$K(\theta_{ijk}) = \frac{1}{k(|\theta_{ijk}|)^2} \frac{\partial k(|\theta_{ijk}|)}{\partial \theta_{ijk}}, \tag{4.4}$$

where $k(|\theta_{ijk}|)$ is depicted in Figure 7(b). In a identical formulation as before, a new compactness controller can be expressed as follows:

$$u_{i3} = -\sum_{i\in\mathcal{N}} \sum_{j\in\mathcal{N}\setminus\{i\}} \sum_{k\in\mathcal{N}\setminus\{i,j\}} \chi'_{ijk} R_{ot}(D_{ij})_i q, \tag{4.5}$$

with

$$\chi'_{ijk}(t) = \begin{cases} K(\theta_{ijk})(\theta_{ijk} - sign(\theta_{ijk})\frac{\pi}{3}), & \text{if } (i,k) \in \mathcal{N}^2_{j,d_2} \setminus \mathcal{N}^2_{j,d_1}, \\ 0, & \text{otherwise.} \end{cases}$$

4.3.2 *Stability Analysis*

The following result holds for a four-agent network.

THEOREM 4.4 Consider $N = 4$ agents described by (2.1), denoted (i, j, k, l) and driven by the control law (4.5). Furthermore, assume an initial configuration as depicted in Figure 7(a), belonging to $\mathscr{I}'(d_1, d_2) = \mathscr{D}(d_2, 3) \cap \mathscr{E}(d_1)$, where agent j is assumed to be central vertex and the initial inter-agent angles are assumed to be non-equal. Then the system will reach a final configuration belonging to $\mathscr{G}(d_1, d_2)$.

Proof. The complete proof is presented in the appendix, Section 9.5. □

Given the structure of $K(\theta_{ijk})$, the proposed solution can be seen as priority based strategy, where small angles have a higher priority (higher $K(\theta_{ijk})$'s value), and large angles a lower one (smaller $K(\theta_{ijk})$'s value). Thus, singular configurations as those studied in Theorem 4.2 can now be appropriately handled.

In this section, we analysed the convergence properties of the proposed compactness controller. Results have been driven for four-agent networks, as a proof of concept of the provided strategy. These results show the potential of these new control protocols for multi-robot scenarios where the connectivity properties of the network are crucial.

5. Sequential Controller

In the sequel, we provide a novel and efficient controller for robot deployment and formation shape control. A *sequential controller*, composed of the two algorithms presented in previous sections, will be given: one part ensuring dispersion; the second one ensuring the minimization inter-agent angles. The proposed structure is illustrated in Figure 8.

5.1 *Preliminaries*

Consider a Connected Triplet where agents are initially closer than a distance d_1. The smallest time instant for which the distance separating two neighbors reaches the threshold distance d_1, for *the first time* and for two edges, is defined as:

$$t^*_{ijk} = \min\{t|\ \beta_{ij}(0), \beta_{jk}(0) < d_1^2, \beta_{ij}(t^*_{ijk}) = \beta_{jk}(t^*_{ijk}) = d_1^2,\ j \in \mathscr{N},\ i \in \mathscr{N}_{j,d_1},\ k \in \mathscr{N}_{j,d_1} \backslash \{i\}\}. \tag{5.1}$$

Furthermore, the smallest time instant for which the previous condition is satisfied, over the all formation, can be formally defined as:

$$t^*_b = \min\{t| \text{ eq. (5.1) is satisfied}\}.$$

Thus, it follows that $t^*_b \geqslant t^*_a$. Keeping in mind previous definitions, the force minimizing inter-agent angles becomes active for each Connected Triplet (i, j, k) at $t = t^*_{ijk}$, see Figure 8. Note that the dispersion algorithm's final configuration corresponds then to the initial set of the compactness algorithm. Thus, define:

$$\mathscr{I}''(d_1, d_2) = \mathscr{D}(d_2, 2) \cap \mathscr{I}(d_1).$$

as the feasible set of initial configurations.

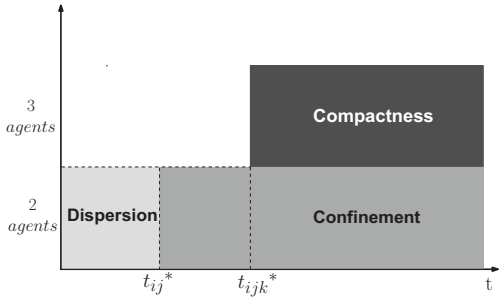


FIG. 8. Sequential controller's time schedule

5.2 *Controller Design*

Due to its nature, the overall control framework can be seen as a hybrid system with transitions at instants when ψ_{ij} is activated and when new edges are added to the graph, or when compactness forces are being applied. Denote agent i's control as

$$u_i = u_{i1} + u_{i2},$$

such that $u = [u_1, \ldots, u_N]^T$. Define now:

$$(R_1)_{pq} = \begin{cases} \displaystyle\sum_{j \in \mathscr{N}\setminus\{p\}} \frac{\partial \gamma_{pj}}{\partial \beta_{pj}}, & \text{if } p = q, \\ \displaystyle -\frac{\partial \gamma_{pq}}{\partial \beta_{pq}}, & \text{otherwise.} \end{cases} \qquad (R_2)_{pq} = \begin{cases} \displaystyle\sum_{j \in \mathscr{N}\setminus\{p\}} \sigma^H_{pj}, & \text{if } p = q, \\ -\sigma^H_{pq}, & \text{otherwise.} \end{cases}$$

and

$$(R_3)_{pq} = \begin{cases} \displaystyle\sum_{j \in \mathscr{N}\setminus\{p\}} \sum_{k \in \mathscr{N}\setminus\{p,j\}} \chi_{pjk}, & \text{if } p = q, \\ \displaystyle\sum_{k \in \mathscr{N}\setminus\{p,q\}} \chi_{pqk}, & \text{otherwise.} \end{cases}$$

In a similar formalization as in [Goebel *et al.* (2009)], we have:

$$\begin{cases} \begin{cases} \dot{q}_i &= -\left[2\alpha((R_1)_i \otimes I_2) + 2\alpha((R_2)_i \otimes I_2)\right] q, \\ \dot{\bar{\theta}}_{ijk} &= \pi, \end{cases} & \text{if } t < t^*_{ijk}, \\ \begin{cases} \dot{q}_i &= -\left[2\alpha((R_1)_i \otimes I_2) + 2\alpha((R_2)_i \otimes I_2) + \lambda((R_3)_i \otimes I_2) R_{ot}\right] q, \\ \dot{\bar{\theta}}_{ijk} &= \theta_{ijk}, \end{cases} & \text{otherwise.} \end{cases} \qquad (5.2)$$

where α and λ are weighting parameters of appropriate dimensions such that $\alpha \gg \lambda$. In other words, dispersion control is prioritized with respect to compactness. It is easy to see that the proposed controller presents an hybrid structure. More precisely, it exhibits both continuous and discrete dynamic behaviors, with jumps described by the evolution of $\bar{\theta}_{ijk}$. Therefore, it follows that the system's state evolves both continuously and discretely.

5.3 *Stability Analysis*

Based on our results presented in Sections 3 and 4, we are going to analyze the proposed sequential controller's performances. The main result of this paper is present in the following.

THEOREM 5.1 Consider $N = 4$ agents (2.1) driven by the control law (5.2). Assume the set of initial conditions $\mathscr{I}''(d_1, d_2)$. Thus, the system reaches a final configuration belonging to $\mathscr{G}(d_1, d_2)$.

Proof. Since the two stages are sequentially related, we consider a global Lyapunov function candidate $V_g(q)$ given by:

$$V_g(q) = \sum_{i \in \mathscr{N}} \sum_{j \in \mathscr{N}\setminus\{i\}} \left[\gamma_{ij} + \psi^H_{ij}\right] + \sum_{j \in \mathscr{N}} \sum_{i \in \mathscr{N}_{j,d_2}} \sum_{k \in \mathscr{N}_{j,d_2}\setminus\{i\}} \left(|\bar{\theta}_{ijk}| - \frac{\pi}{3}\right)^2. \qquad (5.3)$$

For all $t < t_b^*$, $V_g(q)$ corresponds to:

$$V_g(q) = \sum_{i\in\mathscr{N}} \sum_{j\in\mathscr{N}\setminus\{i\}} \left[\gamma_{ij} + \psi_{ij}^H\right] + C_1, \text{ for } t < t_b^*,$$

where $C_1 = \sum_{j\in\mathscr{N}} \sum_{i\in\mathscr{N}_{j,d_2}} \sum_{k\in\mathscr{N}_{j,d_2}\setminus\{i\}} \left(|\bar{\theta}_{ijk}| - \frac{\pi}{3}\right)^2$ is constant (recall the definition of $\bar{\theta}_{ijk}$). Under Assumption 4.1, it follows from Theorem 3.2 that $\dot{V}_g(q)$ is strictly negative. This means that the system will eventually reach a configuration where agents are separated from any other agent within its sensing zone by a distance exactly equal to d_1, and where each agent has at most two neighbors.

At $t = t_b^*$, the compactness controller becomes active for at least one triplet (i,j,k) while the dispersion controller remains active for all agents (i,j) satisfying $\beta_{ij} < d_1^2$. Therefore, we consider the function:

$$V_g(q) = \sum_{j\in\mathscr{N}} \sum_{i\in\mathscr{N}_{j,d_2}} \sum_{k\in\mathscr{N}_{j,d_2}\setminus\{i\}} \left(|\bar{\theta}_{ijk}| - \frac{\pi}{3}\right)^2 + \sum_{i\in\mathscr{N}} \sum_{j\in\mathscr{N}\setminus\{i\}} \left[\gamma_{ij} + \psi_{ij}^H\right], \text{ for } t > t_b^*.$$

In the previous expression, the left hand side term corresponds to the compactness component, which can now be analysed using Lemma 4.1 and Lemma 4.3. Note that, as mentioned before, the controller (5.2) corresponds to a hybrid system where transitions are generated by triplets (i,i,k) that become Connected Triplets (see Definition 2.1) and are incorporated in the definition of $\bar{\theta}_{ijk}$. At each instant $t = t_{ijk}^*$, the value of $\bar{\theta}_{ijk}$ switches from π to the actual value of θ_{ijk} of a triplet (i,j,k). Define $\Delta\bar{\theta}_{ijk} = |\theta_{ijk}| - \pi$. It follows that:

$$\Delta\bar{\theta}_{ijk} < 0, \forall \text{ Connected Triplet } (i,j,k) \ . \tag{5.4}$$

Define also the sum of increments of $V_g(q)$ as $\sum \Delta V_g(q)$, which are related to the switchings on $\bar{\theta}_{ijk}$ values for the different triplets (i,j,k). Thus, it follows from (5.4) that:

$$\sum \Delta V_g(q) < 0, \text{ for } t < t_b^*.$$

Considering Assumption 4.1 and the results of Theorem 3.2 and Lemmas 4.3 and 4.1, we then have:

$$\dot{V}_g(q) < 0, \text{ for } t \in (t_b^*, \infty).$$

Since $\dot{V}_g(q) < 0$ for $t < t_b^*$, $\dot{V}_g(q) < 0$ for $t > t_b^*$, and that all $\Delta V_g(q) < 0$, it follows from Theorem 20 of [Goebel *et al.* (2009)] that the system is asymptotically stable. Agents will eventually reach a configuration belonging to $\mathscr{G}(d_1,d_2)$, where equilateral triangles are formed within the formation and all internal angles are equal to $\pi/3$. This concludes the proof. □

6. Simulation Results

As a main case study, we consider a scenario as illustrated in Figure 1, where a group of robots are deployed to carry out sensing and communication tasks. We are motivated by applications such as intruder detection, search and recover operations or the support to human-driven operations in dangerous environments. For such scenarios, control policies are required to guarantee advanced capabilities for dynamic reconfiguration so to guaranteed performance subject to communication and sensing constraints. We present here simulation results demonstrating that the proposed compact deployment of robots, leading to improved connectivity properties of the swarm, is effective and useful for increased safety, redundancy and efficiency of the measurement and decision-making tasks.

Parameter / Unit	Agent 1	Agent 2	Agent 3	Agent 4	BS	HO
Position (x;y) [m] :						
Case 1	**(1.2; 0.8)**	**(1.3; 1.4)**	**(0.78; 1.91)**	**(1; 2.7)**	**(-4; 1.5)**	**(2.4; -0.4)**
Case 2	**(0.4; 1.5)**	**(1.5; 1.2)**	**(0.5; 1.5)**	**(1.6; 1.3)**	**(-4; 1.5)**	**(2.4; -0.4)**
Number of neighbors (including BS and HO):						
Case 1	**(1+1)**	**(2)**	**(2+1)**	**(1)**	**(1)**	**(1)**
Case 2	**(1+1)**	**(2)**	**(2+1)**	**(1)**	**(2)**	**(0)**

Table 1. Simulation results: parameters and connectivity details for Case 1 and 2.

6.1 *Case study: Mobile sensors/routers deployment*

Consider a static base station (BS), and a swarm of $N = 4$ agents and one human operator (HO) distributed within a constrained environment (e.g., a building or an accident area). In order for the base station to receive measurement data or to transmit relocation orders or warning signals to the robots/human operator, it is important to establish a communication bridge between the different elements. Hence, our goal is to reach a (static) configuration offering increased agent-to-agent, base station-to-agent and human operator-to-base station connectivity. We will pay a particular attention to the resulting configuration and its advantages in what concerns the inter-agent communication links or communication hops between the human operator and the base station. Note that issues related to obstacle avoidance or indoor navigation are outside of the scope of this article, and are not considered here[3].

Table 1 describes the initial conditions for Cases 1 and 2, and the corresponding simulation results are presented in Figure 9. In all figures, the red triangle represents the base station, while the orange square represents the human operator. Moreover, the dashed cones represent the communication ranges for the base station and human operator, the red dashed line $d_2/2$, the blue complete line $d_1/2$, such that $d_1 \simeq d_2 \simeq 1$. Furthermore, in order to better illustrate the concept of compact formations as considered in this article, the resulting triangular pattern is shown in the different figures by the yellow lines.

In Figure 9, the left- and right-hand columns correspond to Case 1 and 2, respectively. In Figure 9(a) one can see that only agent 3 communicates with the base station. Considering that agents can relay information, two communication hops are necessary for information to flow between the base station and agents 2 and 4, three hops to reach agent 1 and up to four hops for information/orders/feedback to reach the human operator. From a connectivity point of view, Case 2 is more challenging: there is no connection between the human operator and the base station, as well as no link between the human operator and the robot swarm, see Figure 9(b).

Figures 9(c) and 9(d) show, for the two cases, the resulting configuration of the dispersion stage. Despite the increased area coverage, where all agents are now at a fixed distance of each other, there are however no clear improvements on the connectivity properties: several hops are still needed for the human operator to communicate with the base station in Case 1, while the human operator remains isolated in Case 2.

Finally, Figures 9(e) and Figure 9(f) show the resulting configuration after the compactness control stage, which offers clear advantages discussed as follows. First, one can see that the number of inter-agent links has increased: all agents have at least two neighbours, and up to four neighbours for agents 1

[3]Note that a potential field based approach could also be used in the future to extend these results, so to guarantee repulsion/attraction with respect to obstacles or the base station/human operator..

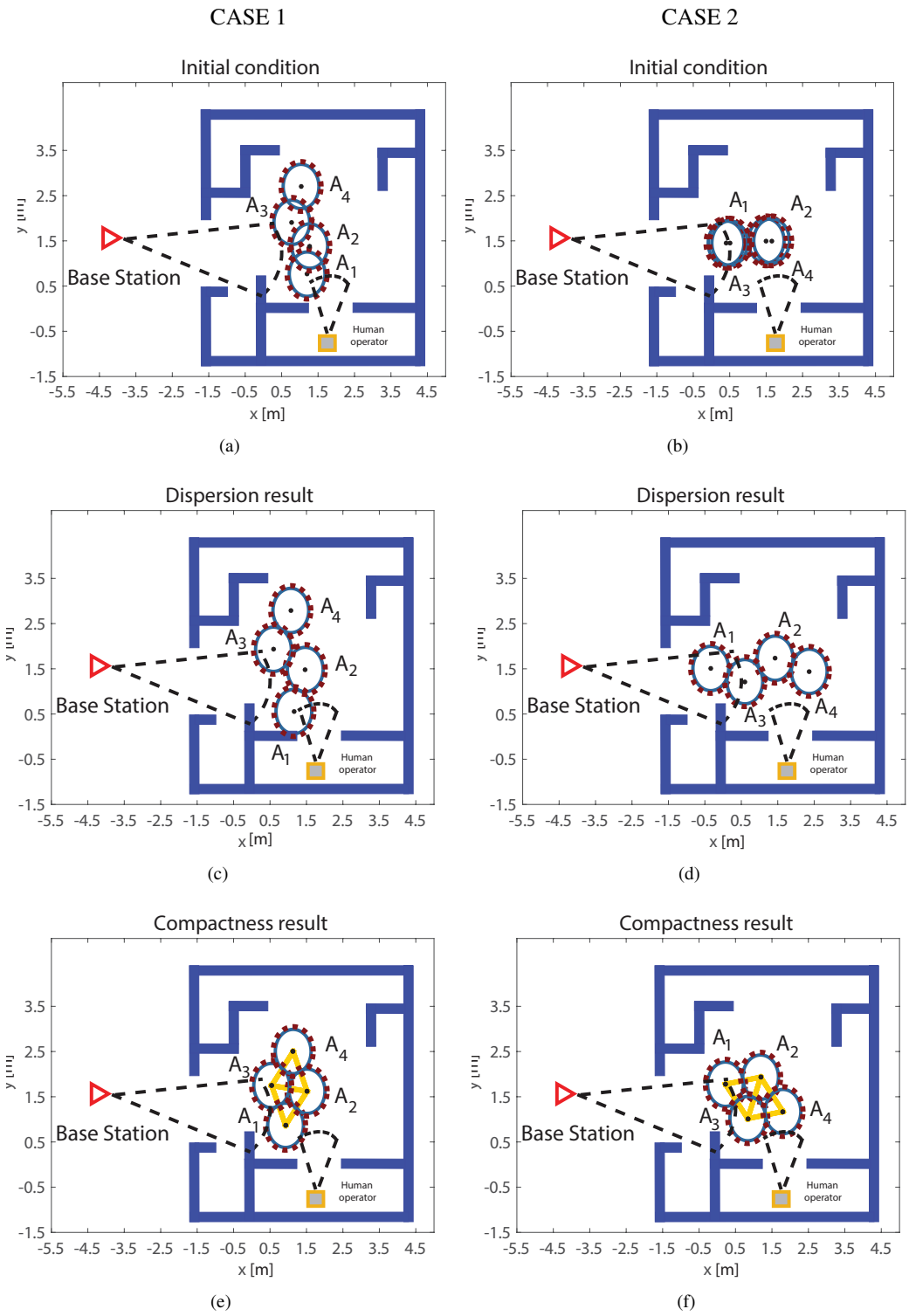


FIG. 9. Simulation results for Case 1 (left-hand side) and Case 2 (right-hand side).

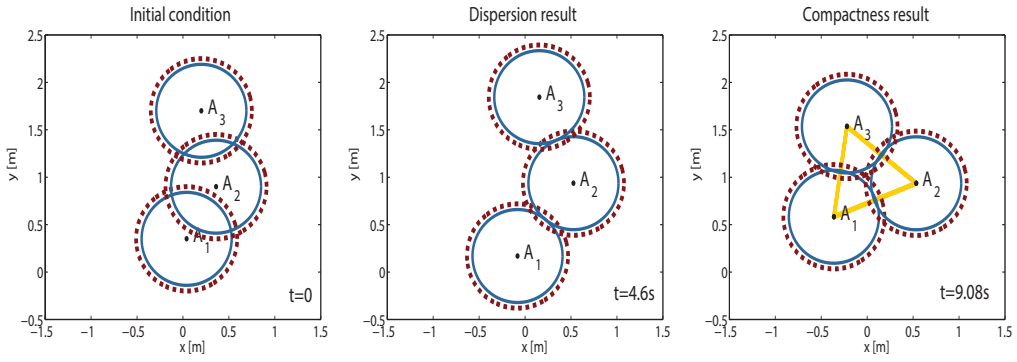
and 3 (including the BS and the HO) in Case 1, for instance. For both Cases 1 and 2, it is also clear that the final configuration offers an improved information flow: information from the base station can reach all agents and the human operator within two hops (instead of the previous four hops for Case 1). Most important, the control of the formation compactness for Case 2 allowed the creation of a link between the human operator and both the swarm and base station, see Figure 9(f). This represents an important improvement with respect to the initial configuration, that dispersion control, if considered independently, would have not been able to achieve.

Parameter / Unit	**Agent 1**	**Agent 2**	**Agent 3**	**Agent 4**
Position (x;y) [m]:				
Case 3	**(0; 0.35)**	**(0.4; 0.9)**	**(0.2; 1.7)**	**–**
Case 4	**(0.1; 2.1)**	**(0.3; 0.9)**	**(0.6; 1.4)**	**(1.2; 1.8)**
Case 5	**(1.1; 1.4)**	**(1.35; 1.5)**	**(1.25; 1.5)**	**–**

Table 2. Simulation results: parameters for Case 3, 4 and 5

6.2 *Particular configurations*

We validate here the results of Theorems 4.2 and 4.3. The simulation parameters for Cases 3 and 4 are given in Table 2. Figure 10 shows the trajectories' evolution for Case 3, i.e., a three agent swarm. One can observe that the final configuration satisfies the control objectives, and that a Complete Triplet has been formed where all agents are separated by a predefined distance. See Figure 10(c). The results corresponding Case 4 are given in Figure 11, and they consider the particular configuration four-agent depicted in Figure 11(a). More precisely, the reader can see in Figure 11(b) the resulting configuration when controller (4.2) is applied. Note that such configuration corresponds to a singular equilibrium where all angles are equal to $2\pi/ = 3$, as studied in Theorem 4.2. Instead, Figure 11(c) shows the resulting formation when the adaptive-gain controller (4.5) is used. Clearly, singular configurations such as the one observed in Figure 11(b) are avoided, and a compact formation achieved.



(a) (b) (c)

FIG. 10. Simulation results for Case 3: a configuration of three agents

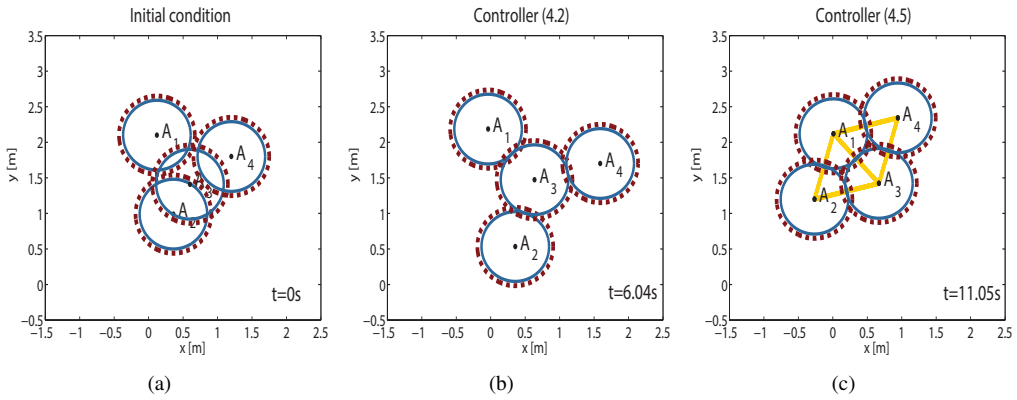


FIG. 11. Simulation results for Case 4: a singular configuration of four agents.

6.3 *Discussion*

The main novelty of this work relies on the mixture of distance-based and angle-based arguments for distributed formation shape control under communication constraints. In order to allow a better understanding of this work, we provide here a brief discussion on its distinctive features and advantages with respect to the existing literature.

Even if distance-based arguments are often used in the literature, as they can generally capture safety and geometric constraints, such approaches are however unable to guarantee compactness, as considered in this paper, for scenarios such as in Figure 10(a) or Figure 6. The same is also true for existing angle-based approaches [Summers *et al.* (2009); Cao *et al.* (2007); Basiri *et al.* (2010); Bishop (2011a)], which assume all-to-all communication graphs or at least an initially formed triangular configuration. While our approach still holds for those cases (see Figure 12), the mentioned solutions are, once again, unable to reach a compact triangular formation from an initial configuration as in Figure 10(a). This comes from the fact that the sensing/communication link between agent 1 and 3 is absent. Another important point is that the existing triangular control approaches do not explicitly consider connectivity and communication/sensing constraints. Hence, connectivity maintenance cannot be explicitly enforced and agents are not guaranteed to maintain suitable distances between them, as illustrated later in Figure 12. Finally, and even if a few of the aforementioned works have been extended to cope with robot swarms of four vehicles, they share the same initial assumptions mentioned before, which makes them unable to cope with configurations such as a connected triplet (Figure 10(a)) or a four agent system such as in Figure 6. Therefore, we propose here a more general set of results that can be applied to a larger set of configurations.

To illustrate some of the aforementioned aspects, we present now some comparative results between the proposed approach and the results of [Bishop (2011a)], which is particularly close to the scope of this work. In [Bishop (2011a)] each agent measures two inter-agent bearings in a local coordinate system and is tasked with establishing and maintaining a desired angular separation relative to its neighbours. According to the paper's own notation, we have prescribed a configuration $\alpha_i^* = \pi/3, \forall\, i$, and considered the original modelling and control setup described in [Bishop (2011a)]. The reader can refer directly to the paper for further details. The simulation parameters for Case 5 are given in Table 2, and the initial configuration is presented in Figure 12 (a), where all agents can sense each other, as requested in [Bishop (2011a)]. In Figure 12 (b) one can see the compact configuration obtained with our sequential

approach. As expected, agents reach an equilateral triangular formation where the internal angles are all equal to $\pi/3$. The configuration in Figure12(c) was obtained using the approach given in [Bishop (2011a)]. While agents reach the prescribed configuration, where all the bearing angles are equal to $\pi/3$, one can however observe that robots travel larger distances in the workspace until they reach a stable, static configuration (see the range of the final positions). As shown in the figure, agents are separated from each other of a distance denoted by d', which is almost fifteen times bigger than d_2 (red, dashed line in the remaining figures). This comes from the fact that the triangular control strategy of [Bishop (2011a)] does not explicitly accounts for communication constrains, and is therefore unable to guarantee connectivity maintenance. For the sake of comparison, the (red delimited) area occupied by the agents in Figure12(b) is also depicted in Figure12(c).

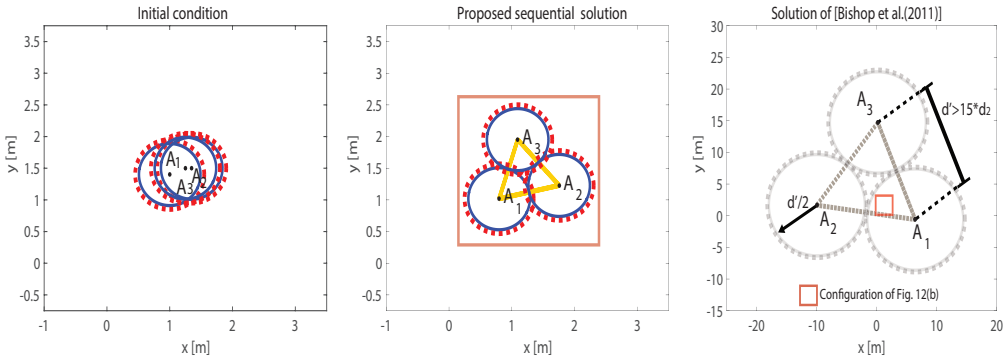


FIG. 12. Simulation results for Case 5: comparison between the proposed sequential solution and the approach of [Bishop (2011a)]. In subfigure (c), the red square region represents the area occupied by the configuration presented in subfigure (b) in the same coordinate frame. This region is meant to highlight the size difference between the resulting configurations. Note that the configuration in subfigure (c) does not satisfy the connectivity constraints any more.

7. Conclusion and Perspectives

We proposed an effective control strategy for the compact deployment of robots. Using angular-based arguments, we showed how to control the compactness of the swarm in order to improve the connectivity properties of the graph. First, we have shown the efficiency of our potential-field based controller that ensures agents' dispersion while keeping the graphs' connectivity and avoiding collisions. Second, we proposed a compactness controller that acts on the inter-agent angles defined within the swarm. Finally, a sequential formulation composed of both the dispersion and compactness control laws was proposed and its stability analysed based on hybrid systems' theory. To improve this work, future research should consider larger systems or the effect of noise on position measurements. Moreover, the proposed framework could also be extended to consider agents with varying and not necessarily common radii, for instance, or cases where agents are moving in the environment.

8. Acknowledgements

This work has been supported by Grenoble INP, the European Commission project FeedNetBack (http://www.feednetback.eu/), the grant AD14VARI02-Progetto ERC BETTER CARS, Chalmers' Area of Advance in Transportation and SAFER.

9. Appendix

9.1 *Proof of Theorem 3.2*

Consider V_d as a Lyapunov function such that:

$$V_d(q) = \sum_{i\in\mathcal{N}} \sum_{j\in\mathcal{N}\setminus\{i\}} \left[\gamma_{ij}(\beta_{ij}) + \psi_{ij}^H(\beta_{ij})\right]. \tag{9.1}$$

For the sake of readability, the argument of the Lyapunov function will be omitted. We compute $\nabla\gamma_{ij} = 2\frac{\partial\gamma_{ij}}{\partial\beta_{ij}} D_{ij} q$ and $\nabla\psi_{ij}^h = 2\frac{\partial\psi_{ij}^h}{\partial\beta_{ij}} D_{ij} q$, and

$$\frac{\partial\gamma_{ij}}{\partial\beta_{ij}} = \frac{\partial\gamma_{ji}}{\partial\beta_{ji}}, \quad \frac{\partial\psi_{ij}}{\partial\beta_{ij}} = \frac{\partial\psi_{ji}}{\partial\beta_{ji}}, \quad \sigma_{ij}^H = \sigma_{ji}^H,$$

due to symmetry. Thus, it follows that:

$$\nabla V_d = \sum_{i\in\mathcal{N}} \sum_{j\in\mathcal{N}\setminus\{i\}} \left[\nabla\gamma_{ij} + \nabla\psi_{ij}^H\right] = 4(R_1\otimes I_2)q + 4(R_2\otimes I_2)q = 4\left[(R_1+R_2)\otimes I_2\right]q.$$

Finally, the derivative of the Lyapunov function can be expressed as:

$$\dot{V}_d = (\nabla V_d)^T \dot{q} = -8\|[(R_1\otimes I_2) + (R_2\otimes I_2)]q\|^2. \tag{9.2}$$

Therefore, $\dot{V}_d$ is strictly negative for all $t > 0$, guaranteeing the system's convergence. Let us discuss this conclusion. Consider any $t < t_a^*$. For any two initially close agents such that $\beta_{ij}(0) < d_1^2, \forall j \in \mathcal{N}_{i,d_1}$, we have $\frac{\partial\gamma_{ij}}{\partial\beta_{ij}} < 0$ if $\beta_{ij} < d_1^2$. Moreover, $\frac{\partial\gamma_{ij}}{\partial\beta_{ij}} = 0$ if $\beta_{ij} \geqslant d_1^2$, and therefore $\beta_{ij} = d_1^2$ corresponds to the equilibrium point of γ_{ij}. Since the contribution of the remaining potential fields is null for $\beta_{ij} < d_1^2$, it follows that for any two agents $\dot{\beta}_{ij} > 0$ such that β_{ij} will eventually reach a close neighborhood of d_1^2. At $t = t_a^*$, the potential function ψ_{ij} is activated for at least one pair of agents. For this pair of agents, two evolution cases are possible: either $\dot{\beta}_{ij} < 0$ such that $(d_1-\eta)^2 < \beta_{ij} < d_1^2$ (situation *[i]*), or $\dot{\beta}_{ij} > 0$ such that $d_1^2 < \beta_{ij} < (d_1+\eta)^2$, (situation *[ii]*):

[i] By definition, if $(d_1-\eta)^2 < \beta_{ij} < d_1^2$, the quantities $\frac{\partial\gamma_{ij}}{\partial\beta_{ij}}$ and $\frac{\partial\psi_{ij}}{\partial\beta_{ij}}$ are strictly negative. This means that throughout (3.2) a repulsive force is applied to agents i and j, and therefore $\dot{\beta}_{ij} > 0$. Moreover, since V_d tends to $+\infty$ whenever β_{ij} tends to $(d_1-\eta)^2$, we can conclude that the distance separating agents will never reach $(d_1-\eta)^2$.

[ii] By definition, if $d_1^2 < \beta_{ij} < (d_1+\eta)^2$, the quantities $\frac{\partial\gamma_{ij}}{\partial\beta_{ij}}$ and $\frac{\partial\psi_{ij}}{\partial\beta_{ij}}$ are equal to zero and strictly positive, respectively. This means that throughout (3.2) an attractive force is applied to agents i and j and therefore $\dot{\beta}_{ij} < 0$. Since V_d tends to ∞ when β_{ij} tend to $(d_1+\eta)^2$, we can conclude that the distance separating agents will never reach $(d_1+\eta)^2$.

Considering the specific design characteristics of ψ_{ij}^H, it follows that if a new edge is created, *i.e.*, if the distance separating agents i and j is lower than a given threshold $d_1+\eta$, the transition between ψ_{ij}^h and ψ_{ij} is held in a sufficiently smooth manner. This means that once an edge is added it is never deleted. Thus, this yields that $V_d(q(t)) \leqslant V_d(q(0))$ for all $t \geqslant 0$ and $V_d \to \infty$ when $\beta_{ij} \to d_1^2 \pm \eta$ for at least one pair of agents (i,j). Then, we can conclude that $q(t) \in \mathscr{F}(d_1,\eta)$ for all $t \geqslant 0$ where all agent pairs that come into distance less or equal to $d_1+\eta$ for the first time, remain within distance $d \in [d_1-\eta, d_1+\eta]$ for all future times. In the sequel, we use LaSalle's Invariance Principle. According to Theorem 3.1, if there exists a Lyapunov function whose derivative along the systems trajectories is negative semidefinite and no trajectory other than the origin can stay identically at points where $\dot{V}_d = 0$, then the origin is asymptotically stable. By LaSalle's Principle, the trajectories of the closed loop system converge to the largest invariant subset of the set:

$$S = \left\{q|\ \dot{V}_d = 0\right\} = \{q|([R_1+R_2]\otimes I_2)q = 0\}\,.$$

Note that within S we have $\dot{q} = u_1 = -2\,[R_1\otimes I_2 + R_2 \otimes I_2]\,q = 0 \Rightarrow u_1 = 0$ for all $i \in \mathscr{N}$, i.e., all agents eventually stop. Due to the invariance of $\mathscr{I}(d_1)$, no trajectory of the closed loop system starting from $\mathscr{I}(d_1)$ can ever leave the set, i.e., $d_1^2 \geqslant \beta_{ij} > 0\ ,\ \forall t \geqslant 0$. Thus, one can conclude that:

$$S_0 = \left\{q|\ \frac{\partial \gamma_{ij}}{\partial \beta_{ij}} = \frac{\partial \psi_{ij}}{\partial \beta_{ij}} = 0,\ \ \forall i,j \in \mathscr{N}, i \neq j\right\}$$

is the largest invariant subset of S. Since $\frac{\partial \gamma_{ij}}{\partial \beta_{ij}} = \frac{\partial \psi_{ij}}{\partial \beta_{ij}} = 0$ only holds when $\beta_{ij} = d_1^2$, then the largest invariant set is the origin and the system will converge to it as $t \to \infty$. This concludes the proof.

□

9.2 *Proof of Theorem 4.1*

From (2.3), one obtain:

$$\frac{\mathrm{d}}{\mathrm{d}\theta_{ijk}}\cos(\theta_{ijk}) = K\left[2(\theta_{ijk} - sign(\theta_{ijk})\frac{\pi}{3}) + (\theta_{jil} - sign(\theta_{jil})\frac{\pi}{3})\right] sin(\theta_{ijk}), \tag{9.3a}$$

$$\frac{\mathrm{d}}{\mathrm{d}\theta_{jil}}\cos(\theta_{jil}) = K\left[2(\theta_{jil} - sign(\theta_{jil})\frac{\pi}{3}) + (\theta_{ijk} - sign(\theta_{ijk})\frac{\pi}{3})\right] sin(\theta_{jil}). \tag{9.3b}$$

Consider V_c as a Lyapunov function candidate defined by:

$$V_c(q) = \sum_{j\in\mathscr{N}}\ \sum_{i\in\mathscr{N}_{j,d_2}}\ \sum_{k\in\mathscr{N}_{j,d_2}\setminus\{i\}} \left(\theta_{ijk} - sign(\theta_{ijk})\frac{\pi}{3}\right)^2.$$

It is worth mentioning that for a set of four agents there are two correlated inter-agent angles to be controlled. The interaction of such angles, sharing one edge, is clearly visible in (9.3). Due to the geometric constraints that $\mathscr{F}'(d_1,d_2)$ implies, $|\theta_{ijk}| \geqslant \pi/3, \forall j \in \mathscr{N}, (i,k) \in \mathscr{N}_{j,d_2}^2, i \neq k$ (since in a isosceles Connected Triplet edges are of length d_1). Thus, either $\pi/3 \leqslant \theta_{ijk} < \pi$ or $-\pi < \theta_{ijk} \leqslant -\pi/3$ such that the function $V_c(q)$ is continuous. Then, $V_c(q) = (\theta_{ijk} - sign(\theta_{ijk})\frac{\pi}{3})^2 + (\theta_{jil} - sign(\theta_{jil})\frac{\pi}{3})^2$. Retrieving $\dot{\theta}_{ijk}$ and $\dot{\theta}_{jil}$ from (9.3), we can write:

$$\dot{V}_c(q) = -4K\left[(\theta_{ijk} - sign(\theta_{ijk})\frac{\pi}{3})^2 + (\theta_{jil} - sign(\theta_{jil})\frac{\pi}{3})^2 + \ (\theta_{ijk} - sign(\theta_{ijk})\frac{\pi}{3})(\theta_{jil} - sign(\theta_{jil})\frac{\pi}{3})\right].$$

Since the right hand side of the previous equation is strictly negative, it follows that $V_c(q(t)) < V_c(q(0)) < \infty$ for all $t \geqslant 0$, and that $|\theta_{ijk}| \to |\theta_{jil}| \to \pi/3$, and inherently, all the Complete Triplet's edges are equal to d_1. This concludes the proof.

□

9.3 *Proof of Theorem 4.2*

Following the same reasoning as before, one can obtain:

$$\frac{\mathrm{d}}{\mathrm{d}\theta_{ijk}}\cos(\theta_{ijk}) = K\left[2(\theta_{ijk} - sign(\theta_{ijk})\frac{\pi}{3}) - (\theta_{jil} - sign(\theta_{jil})\frac{\pi}{3}) - (\theta_{jkm} - sign(\theta_{jkm})\frac{\pi}{3})\right] sin(\theta_{ijk}),$$

$$\frac{\mathrm{d}}{\mathrm{d}\theta_{jil}}\cos(\theta_{jil}) = K\left[2(\theta_{jil} - sign(\theta_{jil})\frac{\pi}{3}) - (\theta_{ijk} - sign(\theta_{ijk})\frac{\pi}{3}) - (\theta_{jkm} - sign(\theta_{jkm})\frac{\pi}{3})\right] sin(\theta_{jil}),$$

$$\frac{\mathrm{d}}{\mathrm{d}\theta_{lji}}\cos(\theta_{lji}) = K\left[2(\theta_{lji} - sign(\theta_{lji})\frac{\pi}{3}) - (\theta_{ijk} - sign(\theta_{ijk})\frac{\pi}{3}) - (\theta_{jil} - sign(\theta_{jil})\frac{\pi}{3})\right] sin(\theta_{lji}).$$

From a geometric point of view, it is obvious that if all agents are sharing the same vertex j, the evolution on an angle is closely dependent on the others such that:

$$2\pi = |\theta_{ijk}| + |\theta_{kjl}| + |\theta_{lji}|. \tag{9.4}$$

Furthermore, if we consider $V_c(q)$ as a Lyapunov function candidate defined by

$$V_c(q) = \sum_{j\in\mathcal{N}} \sum_{i\in\mathcal{N}_{j,d_2}} \sum_{k\in\mathcal{N}_{j,d_2}\setminus\{i\}} \left(|\theta_{ijk}| - \frac{\pi}{3}\right)^2,$$

its derivative can be expressed as:

$$\begin{aligned}\dot{V}_c(q) = -4K\Big[&-(\theta_{ijk} - sign(\theta_{ijk})\frac{\pi}{3})(\theta_{jil} - sign(\theta_{jil})\frac{\pi}{3}) \\ &- (\theta_{ijk} - sign(\theta_{ijk})\frac{\pi}{3})(\theta_{lji} - sign(\theta_{lji})\frac{\pi}{3}) - (\theta_{jil} - sign(\theta_{jil})\frac{\pi}{3})(\theta_{lji} - sign(\theta_{lji})\frac{\pi}{3}) \\ &+ (\theta_{ijk} - sign(\theta_{ijk})\frac{\pi}{3})^2 + (\theta_{jil} - sign(\theta_{jil})\frac{\pi}{3})^2 + (\theta_{lji} - sign(\theta_{lji})\frac{\pi}{3})^2\Big].\end{aligned} \tag{9.5}$$

Define, for the sake of simplicity of notation, $a = (\theta_{ijk} - sign(\theta_{ijk})\frac{\pi}{3})$, $b = (\theta_{jil} - sign(\theta_{jil})\frac{\pi}{3})$ and $c = (\theta_{lji} - sign(\theta_{lji})\frac{\pi}{3})$. The equation (9.5) can be rewritten as:

$$\dot{V}_c(q) = -4K\left[a^2 + b^2 + c^2 - ab - ac - bc\right].$$

The partial derivatives of $\dot{V}_c(q)$ are given by $\frac{\partial \dot{V}_c(q)}{\partial a} = 2a - b - c$, $\frac{\partial \dot{V}_c(q)}{\partial b} = 2b - a - c$ and $\frac{\partial \dot{V}_c(q)}{\partial c} = 2c - a - b$. This yields that $\dot{V}_c(q)$ has an extremum when $\frac{\partial V_c(q)}{\partial a} = \frac{\partial V_c(q)}{\partial b} = \frac{\partial V_c(q)}{\partial c} = 0$, *i.e.*, when $a = b = c$. One can then conclude that $\dot{V}_c(q)$ is a strictly negative function with a global maximum equal to zero when $|\theta_{ijk}| = |\theta_{kjl}| = |\theta_{lji}| = \frac{2\pi}{3}$. This concludes the proof.

□

9.4 *Proof of Theorem 4.3*

Based on the definition of the set $\mathscr{F}'(d_1,d_2)$, the distance separating two connected agents is constant and equal to d_1. From equation (2.3), we can compute:

$$\frac{d}{dt}\cos(\theta_{ijk}) = \frac{\left[< \dot{q_{ji}}, q_{jk} > + < q_{ji}, \dot{q_{jk}} >\right]}{\|q_{ji}\|\,\|q_{jk}\|}. \tag{9.6}$$

We can easily obtain:

$$< q_{ji}, {q_{jk}}^{\perp} >= -\|q_{ji}\|\|q_{jk}\|\sin(\theta_{ijk}), \quad < {q_{ji}}^{\perp}, q_{jk} >= \|q_{ji}\|\|q_{jk}\|\sin(\theta_{ijk}).$$

Considering controller (4.2), (9.6) can be written as:

$$\frac{d}{dt}\cos(\theta_{ijk}) = 2K\left(\theta_{ijk} - sign(\theta_{ijk})\frac{\pi}{3}\right)\sin(\theta_{ijk}).$$

Finally, for all $sin(\theta_{ijk}) \neq 0$ we have:

$$\dot{\theta}_{ijk} = -2K\left(\theta_{ijk} - sign(\theta_{ijk})\frac{\pi}{3}\right).$$

Note that previous manipulations exclude cases where $|\theta_{ijk}| = k\pi$, since otherwise θ_{ijk} is an invalid inter-agent angle According to Assumption 2.1, corresponding to a particular equilibrium offering two possible trajectories. Consider now the following Lyapunov function candidate:

$$V_c(q) = \sum_{j\in\mathscr{N}} \sum_{i\in\mathscr{N}_{j,d_2}} \sum_{k\in\mathscr{N}_{j,d_2}\setminus\{i\}} \left(\theta_{ijk} - sign(\theta_{ijk})\frac{\pi}{3}\right)^2.$$

Note that for each Connected Triplet, there is only one inter-agent angle to be controlled. Due to the geometric constraints that $\mathscr{F}'(d_1,d_2)$ implies, $|\theta_{ijk}| \geqslant \pi/3, \forall j \in \mathscr{N}, (i,k) \in \mathscr{N}^2_{j,d_2}, i \neq k$ (since in a isosceles Connected Triplet edges are at least of length d_1). Thus, either $\pi/3 \leqslant \theta_{ijk} < \pi$ or $-\pi < \theta_{ijk} \leqslant -\pi/3$, which leads us to a continuous function $V_c(q)$. Its derivative can then be written as:

$$\dot{V}_c(q) = -4K\left(\theta_{ijk} - sign(\theta_{ijk})\frac{\pi}{3}\right)^2. \tag{9.7}$$

Thus, $\dot{V}_c(q)$ remains non-positive for all $t \geqslant 0$, so that $|\theta_{ijk}|$ tends to $\pi/3$. Based on geometric arguments, this necessarily means that the third edge's length tends to d_1, and consequently that a Complete Triplet is eventually formed. This concludes the proof.

□

9.5 *Proof of Theorem 4.4*

From its definition, we have $k(|\theta_{ijk}|) > 0$ and $\frac{\partial k(|\theta_{ijk}|)}{\partial|\theta_{ijk}|} \geqslant 0$. Furthermore, it follows from (4.4) that $K(\theta_{ijk})$ value increases as $|\theta_{ijk}| \to \pi/3$. Therefore, for each Connected Triplet (i,j,k), the smaller θ_{ijk}'s value is the stronger the contribution of (4.2) will be. Based on simple geometric arguments, it yields that for a set of four agents in similar formation as in Figure 7(a) there are three controllable inter-agent angles and that their sum is equal to 2π. Under the assumption that the initial inter-agent angles are

not equal, it follows that the absolute value of an inter-agent angle will be strictly inferior to all the others' values such that, for example, $\theta_{ijk} < \theta_{ljk} < \theta_{kjl}$. Since $K(\theta_{ijk})$ value increases as $|\theta_{ijk}| \to \pi/3$, the reader can see in this approach a priority based strategy. In other words, the force applied to small angles has a higher priority (higher $K(\theta_{ijk})$'s value), while large angles have lower priority (smaller $K(\theta_{ijk})$'s value). For the sake of brevity, the rest of the proof can been obtained from the proof of Theorem 4.2 and will therefore be omitted.

□

References

ANDERSON, B., YU, C., DASGUPTA, S. & SUMMERS, T. (2010) Controlling Four Agent Formations, *Proceedings of the* 2 nd *Distributed Estimation and Control in Networked Systems Annecy, France, September 13-14, 2010.*

BASIRI, M., BISHOP, A., & JENSFELT, P. (2010) Distributed control of triangular formations with angle-only constraints, *Systems & Control Letters*, **59** (2), 147–154.

BATALIN, M. & SUKHATME, G. (2002) Spreading out: A local approach to multi-robot coverage, *Proceedings of the* 6 th *International Symposium on Distributed Autonomous Robotics Systems*, 373–382.

BATALIN, M. & SUKHATME, G. (2007) The design and analysis of an efficient local algorithm for coverage and exploration based on sensor network deployment, *IEEE Trans. on Robotics and Automation*, **23** (4), 661–675.

BEARD, R., LAWTON, J. & HADAEGH, F. (2001) A coordination architecture for spacecraft formation control, *IEEE Trans. on Control Systems Technology*, **9** (6), 777–790.

BEZZO, N. & FIERRO, R. (2010) Tethering of mobile router networks, *Proceedings of the American Control Conference*, 6828–6833.

BEZZO, N., YAN, Y., FIERRO, R., & MOSTOFI, Y. (2011) A Decentralized connectivity strategy for mobile router swarms, *Proceedings of the* 18 th *IFAC World Congress*, 4685–4690.

BEZZO N., FIERRO R., SWINGLER A. & FERRARI S. & (2011) A disjunctive programming approach for motion planning of mobile router networks, *International Journal of Robotics and Automation*, **26**(1), 13–25.

BISHOP, A. (2011a) A Very Relaxed Control Law for Bearing-Only Triangular Formation Control ,18th *IFAC World Congress*.

BISHOP, A., SHAMES I., & ANDERSON, B. (2011b) Stabilization of rigid formations with Ddirection-only constraints, *Proceedings of the* 50 th *IEEE Conference on Decision and Control and European Control Conference*, 746–752.

BISHOP, A. & BASIRI M. (2010) Bearing-Only Triangular Formation Control on the Plane and the Sphere, *Mediterranean Conference on Control & Automation*.

BISHOP, A., DEGHAT, M. ANDERSON, B. & HONG, Y. (2015) Distributed formation control with relaxed motion requirements, *International Journal of Robust and Nonlinear Control, **25**(17), 1099–1239* .

BRINON-ARRANZ, L., SEURET, A.,& CANUDAS-DE-WIT, C. (2014) Cooperative Control Design for Time-Varying Formations of Multi-Agent Systems, *IEEE Trans. on Automatic Control*, **59** (8), 2283–2288.

CAO, Z., XIE, L., ZHANG, B., WANG S., & TAN, M. (2003) Formation constrained multi-robot system in unknown environments, *Proceedings of the 2003 IEEE International Conference on Robotics and Automation*, 735–740.

CAO, YONGCAN, STUART, D., WEI REN & ZIYANG MENG CAO (2003) Distributed Containment Control for Multiple Autonomous Vehicles With Double-Integrator Dynamics: Algorithms and Experiments, *IEEE Trans. on Control Systems Technology*, **19** (4), 929–938.

CAO, M., MORSE, A.S., YU, C., ANDERSON, B.D.O., & DASGUPTA, S. (2007) Controlling a triangular formation of mobile autonomous agents, *IEEE Conference on Decision and Control*, 3603-3608.

CAO, M., YU, C., & ANDERSON, B. (2011) Formation control using range-only measurements, *Automatica*, 776-781.

CHEN, J., DONG, S., YANG, J., & CHEN, H. (2010) Leader-follower formation control of multiple non-holonomic mobile Robots Incorporating a Receding-horizon Scheme, *The International Journal of Robotics Research*, **29** (6), 727–747.

CHUANG, Y., YUAN, H. , D'ORSOGNA, M. & BERTOZZI, A. (2007) Multi-vehicle flocking: scalability of cooperative control algorithms using Pairwise Potentials, *Proceedings of the IEEE International Conference on Robotics and Automation*, 2292–2299.

CONSOLINIA, L., MORBIDI, F., PRATTICHIZZO, D., & TOSQUES, M. (2008) Leader-follower formation control of nonholonomic mobile robots with input constraints, *Automatica*, **44** (5), 1343–1349.

CORTÉS, J., MARTÍNEZ, S., KARATAŞ, T., & BULLO, F. (2004) Coverage Control for Mobile Sensing Networks, *IEEE Trans. on Robotics and Automation*, **20** (2), 243–255.

CORTÉS, J., MARTÍNEZ,S. , & BULLO, F. (2006) Robust rendezvous for mobile autonomous agents via proximity graphs in arbitrary dimensions, *IEEE Trans. on Automatic Control*, **51** (8), 1289–1298.

COUZIN, I., KRAUSE, J., FRANKS, N. & LEVIN, S. (2004) Effective leadership and decision-making in animal groups on the move, *Nature*, **433**, 513-516.

DESHPANDE, P., MENON, P., EDWARDS, C. & POSTLETHWAITE, I. (2011) Formation control of multi-agent systems with double integrator dynamics using delayed static output feedback, *IEEE Conference on Decision and Control and European Control Conference*.

DIMAROGONAS, D. & KYRIAKOPOULOS, K. (2007) On the rendezvous problem for multiple nonholonomic agents, *IEEE Trans. on Automatic Control*, **52** (5), 916–922.

DIMAROGONAS, D. & KYRIAKOPOULOS, K. (2007) Inverse agreement protocols with application to distributed multi-agent dispersion, *IEEE Trans. on Automatic Control*, **54** (3), 657–663.

DIMAROGONAS, D. & JOHANSSON, K.H. (2010) Bounded control of network connectivity in multi-agent systems, *IET Control Theory Applications*, **4** (8), 1330–1338.

DONG, W. (2011) Robust formation control of multiple wheeled mobile robots, *Journal of Intelligent & Robotic Systems*, **62** (3), 547–565.

DUDENHOEFFER, D. & JONES, M. (2000) A formation behavior for large-scale micro-robot force deployment, *Proceedings of the Winter Simulation Conference*, 972-982.

EGERSTEDT, M., & XIAOMING, H. (2001) Formation constrained multi-agent control, *IEEE Trans. on Robotics and Automation*, **17** (6), 947–951.

EREN, T. (2012) Formation shape control based on bearing rigidity, *International Journal of Control*, **85** (9), 1361–1379.

FANKHAUSER, B., MAKAREM, L. & GILLET, D. (2011) Collision-free intersection crossing of mobile robots using decentralized navigation functions on predefined paths, 5^{th} *International Conference on Cybernetics and Intelligent Systems*, 392–397.

GAGE, D. (1992) Command control for many-robot systems, *Proceedings of the* 9^{th} *Annual AUVS Technical Symposium,* 28–34.

GAZI, V., & PASSINO, K. (2003) Stability analysis of swarms, *IEEE Trans. on Automatic Control*, **48** (4),692-697.

GHABCHELOO, R., PASCOAL, A., SILVESTRE, C., & KAMINER, I. (2005) Coordinated Path Following Control of Multiple Wheeled Robots with Directed Communication Links, *Proceedings of the* 44^{th} *IEEE Conference on Decision and Control and the European Control Conference*.

GOEBEL, R., SANFELICE, R., & TEEL, A. (2009) Hybrid dynamical systems, *IEEE Control Systems Magazine*, **29** (2), 28–93.

HEXSEL, B., CHAKRABORTY, N. & SYCARA, K. (2011) Coverage control for mobile anisotropic sensor networks, *Proceedings of the IEEE International Conference on Robotics and Automation*, 2878–2885.

HOWARD, A., MATARIC, M., & SUKHATME, G. (2002) An Incremental Self-Deployment Algorithm for Mobile Sensor Networks, *Autonomous Robots, Springer*, **13** (2), 113–126.

JI, M. & EGERSTEDTM, M. (2007) Distributed Connectivity Control of Mobile Networks, *IEEE Trans. on Robotics*, **23** (4), 693–703.

KHALIL, H. (2015) Nonlinear Control, *Pearson Education 2015, ISBN-10: 0-13-349926-X*.

KRUIJFF, G. & JANÍČEK, M. & KESHAVDAS,S. & LAROCHELLE, B. & ET AL. (2007) Experience in system design for human-robot teaming in urban search and rescue, *Field and Service Robotics. Springer*, **23** (4), 111–125.

MAKAREM, L.& GILLET, D. (2012) Fluent coordination of autonomous vehicles at intersections, *International Conference on Systems, Man, and Cybernetics*, 2557–2562.

MANATHARA, J., SUJIT, P. & BEARD, R. (2011) Multiple UAV Coalitions for a Search and Prosecute Mission, *Journal of Intelligent & Robotic Systems*, **62**(1), 125-158.

MARTÍNEZ, S. & BULLO, F. (2006) Optimal sensor placement and motion coordination for target tracking, *Automatica*, **42** (4), 661-668.

MARTÍNEZ, S. , CORTÉS, J. & BULLO, F. (2007) Motion Coordination with Distributed Information, *IEEE Control Systems Magazine*, **27** (214), 75–88.

MASTELLONE, S., STIPANOVIĆ, D., GRAUNKE, C., INTLEKOFER, K. & SPONG, M. (2008) Formation Control and Collision Avoidance for Multi-agent Non-holonomic Systems: Theory and Experiments, *The International Journal of Robotics Research*, **27** (1), 107–126.

MEI,Y., LU, Y., HU, Y., & LEE, C. (2006) Deployment of mobile robots with energy and timing constraints, *IEEE Trans. on Robotics*, **22** (3), 507–522.

MOU S., CAO M., & MORSE A. (2015) Target-point formation control, *Automatica*, **61** (4), 113–118.

OH, K., PARK, M., & AHN, H. (2015) A survey of multi-agent formation control, *Automatica*, **53**, 424–440.

OLFATI-SABER, R. (2006) Flocking for Multi-Agent Dynamic Systems: Algorithms and Theory, *IEEE Trans. on Automatic Control*, **51** (3), 401–420.

PAVONEM, M. & FRAZZOLI, E. (2006) Decentralized Policies for Geometric Pattern Formation and Path Coverage, *Journal of Dynamic Systems, Measurement, and Control*, **129** (5), 633–643.

PODURI, S. & SUKHATME, G. (2009) Constrained coverage for mobile sensor networks, *Proceedings of the IEEE International Conference on Robotics and Automation*, 165–171.

REIF, J. & WANG, H. (2009) Social potential fields: A distributed behavioral control for autonomous robots, *Robotics and Autonomous Systems*, **27** (3), 171–194.

REYNOLDS, C. (1987) Flocks, Herds, and schools: A distributed behavioral model, *Proceedings of the* 14 th *Annual Conference on Computer Graphics and Interactive Techniques,* **4**, 25–34.

REN, W. & BEARD,R. (2008) Distributed Consensus in Multi-vehicle Cooperative Control: Theory and Applications, *Springer London* **4**, 25–34.

RODRIGUES DE CAMPOS, G. & SEURET, A. (2011) Improved consensus algorithms using memory effects , *Proceedings of the IEEE Conference on Decision and Control*.

RODRIGUES DE CAMPOS, G., BRION ARRANZ, L., SEURET, A. & S.-I. NICULESCU (2012) On the consensus of heterogeneous multi-agent systems: a decoupling approach , *Proceedings of the IFAC Workshop on Distributed Estimation and Control in Networked Systems*.

SCHURESKO, M., & CORTÉS, J. (2009) Distributed Motion Constraints for Algebraic Connectivity of Robotic Networks, *Journal of Intelligent & Robotic Systems*, **56** (1), 99–126.

SCHWAGER, M., RUS, D., & SLOTINE, J. (2009) Decentralized, Adaptive Coverage Control for Networked Robots, *The International Journal of Robotics Research*, **9** (3), 357–375.

SEO, S., SHIM, H. & SEO, J. (2011) Finite-time stabilizing dynamic control of uncertain multi-input linear systems, *IMA Journal of Mathematical Control and Information*, **28** (4), 525-537.

SEPULCHRE, R., PALEY, D. & LEONARD, N. (2008) Stabilization of Planar Collective Motion With Limited Communication, *IEEE Trans. on Automatic Control*, **53** (3), 706–719.

SHAMMA, J. (2007) Cooperative control of distributed multi-agent systems, *Wiley Online Library*

SHEN, J. & CAO, J. (2012) Consensus of multi-agent systems on time scales, *IMA Journal of Mathematical Control and Information*, **29** (4), 507-517.

SUMMERS, T.H., CHANGBIN, Y., ANDERSON, B., & DASGUPTA, S. (2009) Formation shape control: Global asymptotic stability of a four-agent formation, *Proceedings of the* 48^{th} *IEEE Conference on Decision and Control*, 3002–3007.

SUN, Z., XIA, Y., & NA, X. (2015) Consensus-based formation control with dynamic role assignment and obstacle avoidance, *IMA Journal of Mathematical Control and Information*.

WEN, G., PENG, Z. YU, Y. & RAHMANI, A. (2013) Planning and control of three-dimensional multi-agent formations, *IMA Journal of Mathematical Control and Information*, **30** (2), 265-284.

ZAVLANOS, M. & PAPPAS, G. (2008) Distributed Connectivity Control of Mobile Networks, *IEEE Trans. on Robotics*, **24** (6), 1416–1428.